Published in final edited form as:
Radiat Res. 2011 December ; 176(6): 842–848.

Cancer-Prone Mice Expressing the Ki-*ras*^{G12C} Gene Show Increased Lung Carcinogenesis after CT Screening Exposures

Michael T. Munley[a,g,1], **Joseph E. Moore**[b], **Matthew C. Walb**[a], **Scott P. Isom**[c,g], **John D. Olson**[d], **J. Gregory Zora**[b], **Nancy D. Kock**[e], **Kenneth T. Wheeler**[f,g], and **Mark Steven Miller**[b,g]

[a]Department of Radiation Oncology, Wake Forest School of Medicine, Medical Center Boulevard, Winston-Salem, North Carolina 27157

[b]Department of Cancer Biology, Wake Forest School of Medicine, Medical Center Boulevard, Winston-Salem, North Carolina 27157

[c]Department of Public Health Sciences, Wake Forest School of Medicine, Medical Center Boulevard, Winston-Salem, North Carolina 27157

[d]Center for Biomolecular Imaging, Wake Forest School of Medicine, Medical Center Boulevard, Winston-Salem, North Carolina 27157

[e]Department of Pathology, Wake Forest School of Medicine, Medical Center Boulevard, Winston-Salem, North Carolina 27157

[f]Department of Radiology, Wake Forest School of Medicine, Medical Center Boulevard, Winston-Salem, North Carolina 27157

[g]Comprehensive Cancer Center of Wake Forest University, Wake Forest School of Medicine, Medical Center Boulevard, Winston-Salem, North Carolina 27157

Abstract

A >20-fold increase in X-ray computed tomography (CT) use during the last 30 years has caused considerable concern because of the potential carcinogenic risk from these CT exposures. Estimating the carcinogenic risk from high-energy, single high-dose exposures obtained from atomic bomb survivors and extrapolating these data to multiple low-energy, low-dose CT exposures using the Linear No-Threshold (LNT) model may not give an accurate assessment of actual cancer risk. Recently, the National Lung Cancer Screening Trial (NLST) reported that annual CT scans of current and former heavy smokers reduced lung cancer mortality by 20%, highlighting the need to better define the carcinogenic risk associated with these annual CT screening exposures. In this study, we used the bitransgenic CCSP-rtTA/Ki-*ras* mouse model that conditionally expresses the human mutant Ki-*ras*^{G12C} gene in a doxycycline-inducible and lung-specific manner to measure the carcinogenic risk of exposure to multiple whole-body CT doses that approximate the annual NLST screening protocol. Irradiated mice expressing the Ki-*ras*^{G12C} gene in their lungs had a significant ($P = 0.01$) 43% increase in the number of tumors/mouse (24.1 ± 1.9) compared to unirradiated mice (16.8 ± 1.3). Irradiated females had significantly ($P < 0.005$) more excess tumors than irradiated males. No tumor size difference or dose response was observed over the total dose range of 80–160 mGy for either sex. Irradiated bitransgenic mice that did not express the Ki-*ras*^{G12C} gene had a low tumor incidence (≤0.1/mouse) that was not affected by exposure to CT radiation. These results suggest that (i) estimating the carcinogenic risk of multiple CT exposures from high-dose carcinogenesis data using the LNT model may be

[1]Address for correspondence: Department of Radiation Oncology, Wake Forest School of Medicine, Medical Center Boulevard, Winston-Salem, NC 27157; mmunley@wfubmc.edu.

inappropriate for current and former smokers and (ii) any increased carcinogenic risk after exposure to fractionated low-dose CT-radiation may be restricted to only those individuals expressing cancer susceptibility genes in their tissues at the time of exposure.

INTRODUCTION

A >20-fold increase in X-ray computed tomography (CT) use during the last 30 years has caused considerable concern because of the potential carcinogenic risk from these CT exposures (1–7). It has been reported that as many as 15,000–45,000 excess tumors are caused by exposure to CT radiation in the U.S. each year (8, 9). However, these estimates are derived from mathematical models that assume that (i) everyone has the same carcinogenic risk after a specific dose of CT radiation, (ii) the carcinogenic risk from multiple low-energy, low-dose (<50 mGy) CT exposures is identical to that of the Japanese atomic bomb survivors, who were exposed predominantly to high-energy, single doses (<2 Gy) of mixed-beam radiation, and (iii) the carcinogenic risk from high-energy, high single-dose data can be extrapolated to multiple low-energy, low-dose CT exposures by the Linear No-Threshold (LNT) model (10, 11). All of these assumptions are required because there are no carcinogenic risk data from low-dose CT exposures to test these assumptions.

Recently, the National Lung Screening Trial (NLST) reported that annual CT scans of 55–74-year-old current and former heavy (≥30 pack years) smokers reduced lung cancer mortality by 20% (12, 13). This result creates a challenge for those responsible for making screening recommendations. On the one hand, annual CT screening of older current and former heavy smokers has the potential to significantly reduce mortality by identifying patients with early-stage localized lung tumors who have approximately a 50% probability of surviving 5 years (14). At present, ~80% of all lung tumors are diagnosed with regional and/or distant spread of disease; these patients have an average probability of < 10% of surviving 5 years (14). Alternatively, annual CT scans of older current and former heavy smokers carry the risk of either initiating normal cells to become tumor cells or promoting the growth of already initiated cells into tumors. This conundrum highlights the need to better define the carcinogenic risk associated with annual CT screening of current and former smokers. This requires testing the assumptions of the mathematical models outlined above by directly measuring excess tumor production after multiple CT exposures in an animal model of current and former smokers.

Adenocarcinoma, a form of non-small cell lung cancer (NSCLC), is the most common histological variant, and its incidence has been increasing (14, 15). In the study reported here, we used a transgenic mouse model developed in our laboratory (16) that contains a mutant form of the human Ki-*ras* gene. Mutations in Ki-*ras* have been implicated as one of the key genetic alterations that drive tumorigenesis in approximately 30% of human lung adenocarcinomas (17–20). The mutant form of the human Ki-*ras* gene was inserted in the mouse genome to create a transgenic mouse in which the mutant human gene is expressed in an inducible and lung-specific manner. This system makes use of the inducible “tet-on” system (21) and involves crossing two different transgenic mice. One transgenic mouse contains a reverse tetracycline (tet) *trans*-activator (rtTA) protein linked to the Clara cell secretory protein (CCSP) promoter. These mice constitutively express the rtTA gene product specifically in the lungs (22). The CCSP-rtTA transgenic mice are crossed with a second transgenic mouse that contains the cDNA of Ki-*ras*^{G12C} cloned into the tetO$_7$-CMV plasmid, placing the mutant Ki-*ras*^{G12C} transgene downstream of a tet-inducible promoter (16). When these two transgenic mice are crossed and treated with doxycycline (DOX), lung-specific expression of the mutant Ki-*ras* transgene product occurs, resulting in the formation of small, benign, hyperplastic foci and very early-stage adenomas that do not

normally progress to more severe tumor types even after a year of continuous DOX treatment (16, 23). We have shown that exposure of DOX-treated mice to lung tumor promoters will result in increased tumor multiplicity and the development of adenocarcinomas (24). Thus our bitransgenic mouse model recapitulates the earliest stages of lung tumor formation and would be representative of asymptomatic smokers and ex-smokers who harbor genetic damage in their lung epithelial cells and contain small, undetectable and relatively benign early-stage lesions. Consequently, this study was designed to evaluate the carcinogenic risk of whole-body multiple CT exposures to asymptomatic smokers and ex-smokers using a protocol that approximates the annual NLST screening protocol (12, 13).

MATERIALS AND METHODS

Mouse Model

All procedures in this study were approved by the institutional animal care and use committee. The bitransgenic CCSP-rtTA/Ki-*ras* mice used in these experiments were generated on an FVB/N background and expressed the Ki-*ras*^{G12C} gene in a doxycycline (DOX)-inducible and lung-specific manner (16). Mice treated with 500 μg/ml of DOX in their drinking water have extensive epithelial hyperplasia of the alveolar region of the lungs and have an average of approximately 20 well-differentiated adenomas/mouse by 9–12 months (16). The lung morphology of CCSP-rtTA/Ki-*ras* mice that do not receive DOX and do not express the transgene is normal. All of the mice were maintained on an AIN-76 diet.

CT Dosimetry and Irradiation Procedures

Mice were irradiated using a clinical multi-detector row (8-slice) helical CT scanner (Fig. 1). This unit is routinely used for radiation therapy treatment planning and has quality assurance performed daily to verify geometric and image intensity accuracy. Dosimetry measurements were made with an ion chamber calibrated at several energies ranging from 30–150 kVp. This ion chamber was placed inside tissue-equivalent material having a diameter of 2.8 cm to approximate the diameter of a mouse. A phantom mouse made of tissue-equivalent material was positioned in the CT scanner next to the ion chamber using the localization lasers (red crosshairs, Fig. 1). This accounted for the scatter dose that occurred when two mice were irradiated at the same time. The doses (5, 15 or 25 mGy/fraction) were delivered to the whole body of each mouse using the CT screening parameters in Fig. 1 and adjusting the tube current to obtain the desired doses.

Experimental Design

Eight groups of 12 CCSP-rtTA/Ki-*ras* mice were entered into the experiment as follows: Group 1: No DOX, sham irradiation; Group 2: No DOX + 5 mGy/fraction; Group 3: No DOX + 15 mGy/fraction; Group 4: No DOX + 25 mGy/fraction; Group 5: DOX + 5 mGy/fraction; Group 6: DOX + 15 mGy/fraction; Group 7: DOX + 25 mGy/fraction; Group 8: DOX + sham irradiation. Each group had approximately the same number of males and females. The timeline for the experiment is shown in Fig. 2.

At 8 weeks of age, the mice in Groups 5–8 began receiving 500 μg/ml of DOX in their drinking water. Beginning at 9 weeks of age, mice were lightly anesthetized with 90 mg/kg of ketamine/10 mg/kg of xylazine and whole-body irradiated in the CT scanner once/week for 4 weeks. Usually two mice were irradiated at a time, but if only one mouse was irradiated, the phantom was placed next to the mouse to ensure that the scatter dose was similar to the two-mouse setup (Fig. 1A). The weekly irradiation schedule was selected to approximate the annual lung screening protocol of the NLST in a short-lived mouse model.

At 3, 6 and 9 months after the last radiation fraction, tumor growth was monitored by CT imaging (30 mGy/exposure) (25–27). At 9 months after the last radiation fraction, the ~1-year-old mice were euthanized, the lungs were removed, and the numbers of tumors and their sizes were determined (16, 23, 24). The lungs were then fixed in Methacarn (methanol/chloroform/acetic acid, 6:3:1) for 48 h, embedded in paraffin, serially sectioned, stained with hematoxylin/eosin, and classified by a blinded board-certified veterinary pathologist using standard murine pulmonary tumor characteristics (28).

Statistical Analysis

Generalized Estimating Equations were used to model the effects of radiation and sex on the number of tumors. The variance of the tumor counts was substantially larger than the mean, leading to the use of the negative binomial distribution with a log link to model the tumor counts. Model-adjusted means were then produced to describe the differences found between the control group and the irradiated groups. The analysis of tumor size was performed using a log transformation to normalize the size values. Statistical significance was set at $P < 0.05$.

RESULTS

Monitoring the effect of multiple CT exposures on the tumor latency and growth required that tumor size be measured noninvasively over the 9-month postirradiation period. When this study began, CT imaging was the only validated technique available at our institution to accomplish this. Given that the 9-month CT imaging procedure was performed just before the mice were euthanized, only the imaging procedures at 3 and 6 months postirradiation could affect the tumor number and size measured at 9 months postirradiation. The four weekly whole-body exposures of 5, 15 or 25 mGy plus the lung imaging exposures of 30 mGy at 3 and 6 months resulted in total lung doses of 80 mGy (Groups 2, 5), 120 mGy (Groups 3, 6), and 160 mGy (Groups 4, 7). Consequently, these total dose values, rather than the sum of the weekly exposures, were used to describe these data.

In this mouse model, two or more tumors can grow together to form a single large lesion defined as a coalesced tumor. In this study, < 8% of the total tumors were coalesced in any single group, and their frequency did not differ between groups or genders. Thus all coalesced tumors were censored before performing the statistical analyses.

In the DOX alone group, there was no significant difference ($P > 0.3$) in the number of tumors found in males and females. Combining all of the data for irradiated males and females revealed an increase in the number of tumors at each of the total doses investigated (Fig. 3A). No significant ($P > 0.1$) dose response was observed, so all of the radiation data were combined for the subsequent analyses. The number of tumors/mouse (24.1 ± 1.9) in irradiated mice expressing the Ki-*ras*^{G12C} gene in their lungs was 43% greater than the number of tumors/mouse (16.8 ± 1.3) in the unirradiated mice expressing the Ki-*ras*^{G12C} gene in their lungs (Fig. 3B; $P = 0.01$). In contrast, the tumor incidence in irradiated (4 tumors in 38 mice) and unirradiated (1 tumor in 12 mice) mice that did not express the Ki-*ras*^{G12C} transgene was identical (Fig. 3B). Thus the increased carcinogenic risk from CT exposures appears to require expression of the Ki-*ras*^{G12C} gene.

For those mice expressing the Ki-*ras*^{G12C} gene, irradiated females had significantly ($P < 0.005$) more tumors/mouse (25.8 ± 2.2) than irradiated males (18.3 ± 1.7; Fig. 4). This observation is consistent with other data showing that females are often more radiosensitive than males (2, 4, 29, 30).

No significant difference ($P > 0.3$) in tumor size was observed between irradiated and unirradiated mice expressing the Ki-*ras*^{G12C} gene in their lungs (Fig. 5). There was also no evidence to suggest that exposure to low-dose CT radiation affected the tumor growth rate (volume doubling time: sham-irradiated = 2.1 months, irradiated = 2.2 months) or morphology (Fig. 6). Although initiation cannot be completely ruled out as contributing to the observed excess tumor formation, these data suggest that (i) the increased number of lung tumors found in irradiated mice expressing the Ki-*ras*^{G12C} gene is likely due to promotion, and (ii) estimating the carcinogenic risk of multiple CT exposures from high-dose carcinogenesis data using the LNT model may be inappropriate for current and former smokers.

DISCUSSION

The most recent evaluation of the carcinogenic risks associated with low doses of ionizing radiation was undertaken by the National Academies' 7th committee on the Biological Effects of Ionizing Radiation. Their task was to update risk estimates for exposures to low doses (< 100 mGy) of low-LET radiation such as CT X rays. In their BEIR VII report, the relative risk of solid cancers, averaged over the sexes, 30 years after exposure at 30 years of age was adequately fitted by the LNT model (10). This conclusion is consistent with ionizing radiation being an initiator where the carcinogenic risk is the result of stochastic events. However, the committee also cautioned that genetic variation in a population is potentially an important factor in estimating cancer risk. In an at-risk population, radiation may act as a promoter whereby once promotion has occurred, additional doses of radiation would not necessarily increase the risk (31–33). In this case, the LNT model would not predict the carcinogenic risk from low-dose exposures (4, 34).

Since BEIR VII, several estimates of the annual excess cancers produced by CT exposures have been published (8, 9). Consistent with the BEIR VII guidelines, these estimates of 15,000–45,000 excess cancers annually have been derived with mathematical models that (i) extrapolate high single-dose data to low-dose CT exposures using the LNT model and (ii) do not account for the potential impact of sex and genetic variation on these risk estimates (10). However, the recent results from the NLST where chest X-ray screening did not reduce lung cancer mortality, while CT screening reduced it by 20%, require a re-examination of these assumptions (12, 13). When compared to the populations receiving CT scans to diagnose injuries or diseases other than cancer, the population being screened for lung cancer has several unique characteristics that could drastically alter their carcinogenic risk estimates.

The lungs of 55–74-year-old current and former heavy smokers likely have many initiated cells that are progressing or are ready to progress to premalignant or malignant lesions. Thus promotion could have a far greater impact on the carcinogenic risk estimates after screening this population with CT. It has been estimated that ~30% of human lung adenocarcinomas have a mutant Ki-*ras* gene. In our study, the bitransgenic CCSP-rtTA/Ki-*ras* mouse has the human mutant Ki-*ras*^{G12C} gene conditionally expressed only in the lungs, as might be expected in current and former heavy smokers. Although the total CT doses ranging from 80–160 mGy resulted in a 43% increase in the number of tumors/mouse (Fig. 3B), (i) the absence of a dose response (Fig. 3A), (ii) no increase in tumorigenesis in the group of mice not treated with DOX that lack upregulation of the mutant Ki-*ras* gene, and (iii) no tumor size difference between the irradiated and unirradiated mice at 9 months after the last weekly fraction (Fig. 5) suggest that promotion, rather than initiation, is the likely mechanism predominantly responsible for the observed increase in tumor number in the DOX-treated mice.

If initiation was the predominant mechanism responsible for the tumor increase in the irradiated mice, we would have expected that many of the tumors observed at 9 months after the last weekly fraction would have been produced by the 30-mGy CT imaging doses at 3 and 6 months postirradiation. If many of the tumors were initiated at 3 and 6 months postirradiation, the average tumor size for the irradiated mice should have been less at 9 months than that for the unirradiated mice, which is not what was observed (Fig. 5). Thus our results are consistent with the hypothesis that (i) promotion is the primary mechanism responsible for the increased tumor number in irradiated mice expressing the Ki-*ras*^{G12C} gene and (ii) most, if not all, of this promotion occurred during the four weekly exposures (total doses of 20–100 mGy).

The critical role of inflammation in mediating cancer progression has been documented in a number of epidemiological and animal studies (35–37). Several studies have shown that pulmonary inflammation is associated with elevated levels of lung tumorigenesis in both murine and human tumors (38–41). Activation of the NF-κB pathway and its downstream effector molecules enhances the production of reactive oxygen species (ROS) and stimulates signal transduction pathways that regulate cell proliferation, cell survival, immune surveillance and angiogenesis (42, 43), thus causing additional genetic and/or epigenetic alterations in postinitiated cells that lead to malignant tumor formation. However, the steps leading from an initiated cell to visible neoplasia still have not been clearly elucidated. In the present study, inflammation may have played a role in the observed radiation-induced increase in lung tumorigenesis; however, that role will need to be defined in future studies.

Interpretation of these results for lung cancer CT screening programs must be tempered by the limitations of our study. First, we have studied only one gene associated with human lung cancer, and that gene is found in only ~30% of human lung adenocarcinomas. Similar studies with other genetic models of human cancer should be performed to confirm these results. Second, the use of CT imaging at 3, 6 and 9 months postirradiation to monitor tumor latency and growth complicated interpretation of the data. We can now perform 7T small animal magnetic resonance imaging (MRI) and have confirmed that tumor sizes measured at 9 months postirradiation by electronic calipers, CT and MRI are identical. Thus MRI can be used in subsequent experiments to avoid the complication of CT imaging. Third, although no dose response was observed, the dose range of 80–160 mGy was relatively small, 38–75% of the total dose came from the imaging procedures, and the dose at which the putative threshold begins was not defined. Fourth, although the difference between the male and female response was highly significant ($P < 0.005$), the numbers were relatively small in each irradiated group. Recently we initiated an experiment using larger numbers of male and female CCSP-rtTA/Ki-*ras* mice, single CT doses of 1.25–80 mGy, and MRI to more definitively assess whether (i) a threshold for tumor formation occurs in this model and (ii) CT radiation affects tumor latency and growth. Finally, it should also be pointed out that our CT screening studies were carried out in young adult mice while middle-aged and older individuals are the likely subjects for lung tumor screening in the clinic. Future studies will be designed to assess the effect of age on radiation-induced tumor formation in this animal model.

Within the limitations described above, our data suggest that (i) individuals expressing one or more cancer susceptibility genes have a higher carcinogenic risk from CT exposures, (ii) individuals not expressing a cancer susceptibility gene have little or no carcinogenic risk from CT exposures, (iii) the increased carcinogenic risk from CT exposures is likely due to promotion rather than initiation, and (iv) estimates of the carcinogenic risk from CT imaging that extrapolate Japanese atomic bomb survivor data (likely initiation) to low-dose CT exposures (likely promotion) using the LNT model should be viewed with caution. Until more definitive data are available, it may be prudent for cancer CT screening programs to

use MRI procedures for individuals expressing cancer susceptibility genes or for individuals who need follow-up imaging of suspicious lesions identified by an initial CT examination. Finally, these data suggest that the carcinogenic risk from whole-body backscatter scanners presently being used to screen passengers at airports may be underestimated for at-risk populations (44, 45).

Acknowledgments

This study was supported by National Cancer Institute grant R01-CA136910 (to MTM), the Wake Forest University Cancer Center Support Grant P30-CA12197, and a Partner Grant from the Comprehensive Cancer Center and the Department of Radiation Oncology at the Wake Forest University School of Medicine. MCW was partially supported by the Dalton L. McMichael, Sr. Fund in Cancer Research. The authors thank Michael E. Robbins, Ph.D., for his critical review of this manuscript.

References

1. Brenner DJ, Hall EJ. Computed tomography—an increasing source of radiation exposure. N Engl J Med. 2007; 357:2277–84. [PubMed: 18046031]
2. Einstein AJ, Henzlova MJ, Rajagopalan S. Estimating risk of cancer associated with radiation exposure from 64-slice computed tomography coronary angiography. JAMA. 2007; 298:317–23. [PubMed: 17635892]
3. Dauer LT, Brooks AL, Hoel DG, Morgan WF, Stram D, Tran P. Review and evaluation of updated research on the health effects associated with low-dose ionising radiation. Radiat Prot Dosimetry. 2010; 140:103–36. [PubMed: 20413418]
4. Shuryak I, Sachs RK, Brenner DJ. Cancer risks after radiation exposure in middle age. J Natl Cancer Inst. 2010; 102:1628–36. [PubMed: 20975037]
5. Mossman KL. Economic and policy considerations drive the LNT debate. Radiat Res. 2008; 169:245–7. [PubMed: 18220464]
6. Leonard BE. Common sense about the linear no-threshold controversy—give the general public a break. Radiat Res. 2008; 169:245–6. [PubMed: 18220465]
7. Feinendegen LE, Paretzke H, Neumann RD. Two principal considerations are needed after low doses of ionizing radiation. Radiat Res. 2008; 169:247–8. [PubMed: 18220467]
8. Brenner DJ. Radiation risks potentially associated with low-dose CT screening of adult smokers for lung cancer. Radiology. 2004; 231:440–5. [PubMed: 15128988]
9. Berrington de Gonzalez A, Mahesh M, Kim KP, Bhargavan M, Lewis R, Mettler F, et al. Projected cancer risks from computed tomographic scans performed in the United States in 2007. Arch Intern Med. 2009; 169:2071–7. [PubMed: 20008689]
10. Health risks from exposure to low levels of ionizing radiation: BEIR VII Phase. Vol. 2. Washington, DC: National Academies Press; 2006. National Research Council Committee to Assess Health Risks from Exposure to Low Levels of Ionizing Radiation.
11. Brenner DJ, Doll R, Goodhead DT, Hall EJ, Land CE, Little JB, et al. Cancer risks attributable to low doses of ionizing radiation: assessing what we really know. Proc Natl Acad Sci U S A. 2003; 100:13761–6. [PubMed: 14610281]
12. National Lung Screening Trial Research Team. The National Lung Cancer Screening Trial: Overview and Study Design. National Lung Screening Trial Research Team Radiology. 2011; 258:243–53.
13. National Lung Screening Trial: Questions and Answers. NCI Cancer Bulletin. 2010. [updated 2010 Nov 26, cited 2011 Apr 13] Available from: http://www.cancer.gov/newscenter/qa/2002/nlstqaQA
14. Jemal A, Siegel R, Xu J, Ward E. Cancer statistics, 2010. CA Cancer J Clin. 2010; 60:277–300. [PubMed: 20610543]
15. Alberg, AJ.; Samet, JM. Epidemiology of lung cancer. In: Kane, MA.; Bunn, PA., Jr, editors. Biology of lung cancer. New York: Marcel Dekker; 1998. p. 11-51.
16. Floyd HS, Farnsworth CL, Kock ND, Mizesko MC, Little JL, Dance ST, et al. Conditional expression of the mutant Ki-*ras*^{G12C} allele results in formation of benign lung adenomas:

Development of a novel mouse lung tumor model. Carcinogenesis. 2005; 26:2196–206. [PubMed: 16051643]

17. Li ZH, Zheng J, Weiss LM, Shibata D. c-K-ras and p53 mutations occur very early in adenocarcinoma of the lung. Am J Pathol. 1994; 144:303–9. [PubMed: 8311114]
18. Westra WH, Slebos RJ, Offerhaus GJ, Goodman SN, Evers SG, Kensler TW, et al. K-ras oncogene activation in lung adenocarcinomas from former smokers. Evidence that K-ras mutations are an early and irreversible event in the development of adenocarcinoma of the lung. Cancer. 1993; 72:432–8. [PubMed: 8319174]
19. Westra WH, Baas IO, Hruban RH, Askin FB, Wilson K, Offerhaus GJ, et al. K-ras oncogene activation in atypical alveolar hyperplasias of the human lung. Cancer Res. 1996; 56:2224–8. [PubMed: 8616876]
20. Reynolds, SH.; Wiest, JS.; Devereux, TR.; Anderson, MW.; You, M. Protooncogene activation in spontaneously occurring and chemically induced rodent and human lung tumors. In: Klein-Szanto, AJP.; Anderson, MW.; Barrett, JC.; Slaga, TJ., editors. Comparative molecular carcinogenesis. New York: Wiley-Liss; 1992. p. 303-20.
21. Shockett PE, Schatz DG. Diverse strategies for tetracycline-regulated inducible gene expression. Proc Natl Acad Sci U S A. 1996; 93:5173–6. [PubMed: 8643548]
22. Hayashida S, Harrod KS, Whitsett JA. Regulation and function of CCSP during pulmonary Pseudomonas aeruginosa infection in vivo. Am J Physiol Lung Cell Mol Physiol. 2000; 279:L452–9. [PubMed: 10956619]
23. Dance-Barnes ST, Kock ND, Floyd HS, Moore JE, Mosley LJ, D'Agostino RB Jr, et al. Effects of mutant human Ki-ras(G12C) gene dosage on murine lung tumorigenesis and signaling to its downstream effectors. Toxicol Appl Pharmacol. 2008; 231:77–84. [PubMed: 18565564]
24. Dance-Barnes ST, Kock ND, Moore JE, Lin EY, Mosley LJ, D'Agostino RB Jr, et al. Lung tumor promotion by curcumin. Carcinogenesis. 2009; 30:1016–1023. [PubMed: 19359593]
25. Schuster DP, Kovacs A, Garbow J, Piwnica-Worms D. Recent advances in imaging the lungs of intact small animals. Am J Respir Cell Mol Biol. 2004; 30:129–38. [PubMed: 14729505]
26. Jennings-Gee JE, Moore JE, Xu M, Dance ST, Kock ND, McCoy TP, et al. Strain-specific induction of murine lung tumors following in utero exposure to 3-methylcholanthrene. Mol Carcinog. 2006; 45:676–84. [PubMed: 16652375]
27. Kennel SJ, Davis IA, Branning J, Pan H, Kabalka GW, Paulus MJ. High resolution computed tomography and MRI for monitoring lung tumor growth in mice undergoing radioimmunotherapy: correlation with histology. Med Phys. 2000; 27:1101–7. [PubMed: 10841415]
28. Nikitin AY, Alcaraz A, Anver MR, Bronson RT, Cardiff RD, Dixon D, et al. Classification of proliferative pulmonary lesions of the mouse: recommendations of the mouse models of human cancers consortium. Cancer Res. 2004; 64:2307–16. [PubMed: 15059877]
29. Goldsby RE, Liu Q, Nathan PC, Bowers DC, Yeaton-Massey A, Raber SH, et al. Late-occurring neurologic sequelae in adult survivors of childhood acute lymphoblastic leukemia: a report from the Childhood Cancer Survivor Study. J Clin Oncol. 2010; 28:324–31. [PubMed: 19917844]
30. Kaste SC, Waszilycsak GL, McCarville MB, Daw NC. Estimation of potential excess cancer incidence in pediatric 201Tl imaging. AJR Am J Roentgenol. 2010; 194:245–9. [PubMed: 20028929]
31. Shuryak I, Ullrich RL, Sachs RK, Brenner DJ. The balance between initiation and promotion in radiation-induced murine carcinogenesis. Radiat Res. 2010; 174:357–66. [PubMed: 20726716]
32. Curtis SB, Luebeck EG, Hazelton WD, Moolgavkar SH. The role of promotion in carcinogenesis from protracted high-LET exposure. Phys Med. 2001; 17 (Suppl 1):157–60. [PubMed: 11771544]
33. Curtis SB, Hazelton WD, Luebeck EG, Moolgavkar SH. From mechanisms to risk estimation—bridging the chasm. Adv Space Res. 2004; 34:1404–9. [PubMed: 15881782]
34. Scott BR. Low-dose radiation risk extrapolation fallacy associated with the linear-no-threshold model. Hum Exp Toxicol. 2008; 27:163–8. [PubMed: 18480143]
35. Hussain SP, Hofseth LJ, Harris CC. Radical causes of cancer. Nat Rev Cancer. 2003; 3:276–85. [PubMed: 12671666]
36. Klaunig JE, Kamendulis LM. The role of oxidative stress in carcinogenesis. Annu Rev Pharmacol Toxicol. 2004; 44:239–67. [PubMed: 14744246]

37. Malkinson AM. Role of inflammation in mouse lung tumorigenesis: a review. Exp Lung Res. 2005; 31:57–82. [PubMed: 15765919]

38. Witschi H, Williamson D, Lock S. Enhancement of urethan tumorigenesis in mouse lung by butylated hydroxytoluene. J Natl Cancer Inst. 1977; 58:301–5. [PubMed: 833878]

39. Cohen BH, Diamond EL, Graves CG, Kreiss P, Levy DA, Menkes HA, et al. A common familial component in lung cancer and chronic obstructive pulmonary disease. Lancet. 1977; 2:523–6. [PubMed: 95731]

40. Tockman MS, Anthonisen NR, Wright EC, Donithan MG. Airways obstruction and the risk for lung cancer. Ann Intern Med. 1987; 106:512–8. [PubMed: 3826952]

41. Keith RL, Miller YE, Hoshikawa Y, Moore MD, Gesell TL, Gao B, et al. Manipulation of pulmonary prostacyclin synthase expression prevents murine lung cancer. Cancer Res. 2002; 62:734–40. [PubMed: 11830527]

42. Karin M. NF-kappaB and cancer: Mechanisms and targets. Mol Carcinog. 2006; 45:355–61. [PubMed: 16673382]

43. Lu H, Ouyang W, Huang C. Inflammation, a key event in cancer development. Mol Cancer Res. 2006; 4:221–33. [PubMed: 16603636]

44. Hupe O, Ankerhold U. X-ray security scanners for personnel and vehicle control: dose quantities and dose values. Eur J Radiol. 2007; 63:237–41. [PubMed: 17628378]

45. Rez P, Metzger RL, Mossman KL. The dose from Compton backscatter screening. Radiat Prot Dosimetry. 2011; 145:75–81. [PubMed: 21068018]

A

B

Energy	100 kVp
Tube current	40, 120, 200 mA
Time	1 sec/revolution
Slice thickness	1.25 mm
Field-of-view	200 mm
Image grid	512 x 512 pixels
Pixel size	0.3906 mm
Pitch	0.75:1
Speed	3.75 mm/rotation
Dose/fraction	5, 15, 25 mGy

FIG. 1.

Irradiation setup and parameters. Panel A: Position of one mouse and the phantom prior to starting irradiation. Panel B: CT irradiation parameters. The three doses were obtained by adjusting the tube current. The irradiation time was ~30 s for all doses.

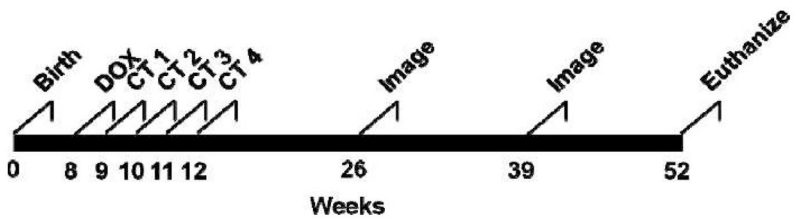

FIG. 2.

Experimental timeline. At 8 weeks of age, groups of 12 bitransgenic CCSP-rtTA/Ki-*ras* mice were entered into the experiment. Half of the groups were given 500 μg/ml of doxycycline (DOX) in their drinking water; the other half were given normal drinking water. One week after initiating the DOX treatment, DOX or No DOX mice were lightly anesthetized and either sham-irradiated or irradiated once each week for 4 weeks with 5, 15 or 25 mGy of 100 kVp X rays from a clinical helical CT scanner. At 3, 6 and 9 months after the last weekly fraction, the lungs were imaged with CT (30 mGy/image) to noninvasively determine the size of the tumors. At 12 months of age the mice were euthanized, the lungs were excised, and the tumors were counted and sized.

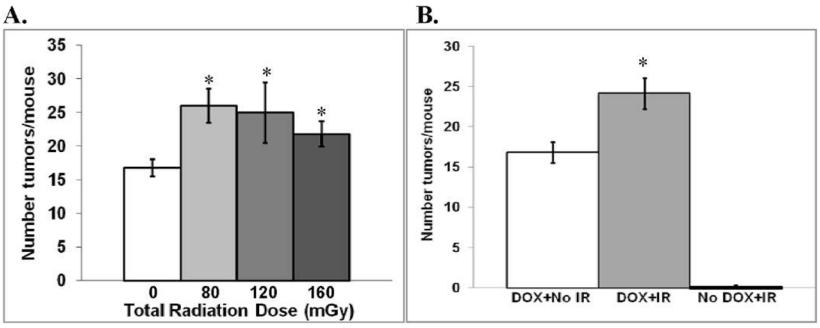

FIG. 3.

Tumor formation with and without CT irradiation. Panel A: Mean number (± SEM) of lung tumors/mouse for each total dose level. There was a significant radiation effect that was independent of dose. **P* < 0.05 compared to unirradiated mice expressing the Ki-*ras*^{G12C} gene. Panel B: Comparison of the mean number of lung tumors/mouse for the combined data for irradiated mice. IR = ionizing radiation. White bar: unirradiated mice expressing the Ki-*ras*^{G12C} gene; gray bar: irradiated mice expressing the Ki-*ras*^{G12C} gene. **P* = 0.01 compared to unirradiated mice expressing the Ki-*ras*^{G12C} gene. Black bar: irradiated mice not expressing the Ki-*ras*^{G12C} gene.

FIG. 4.

Comparison of the number of lung tumors/mouse (mean ± SEM) for irradiated female and male mice expressing the Ki-*ras*^{G12C} gene after combining all of the irradiated groups (*P < 0.005).

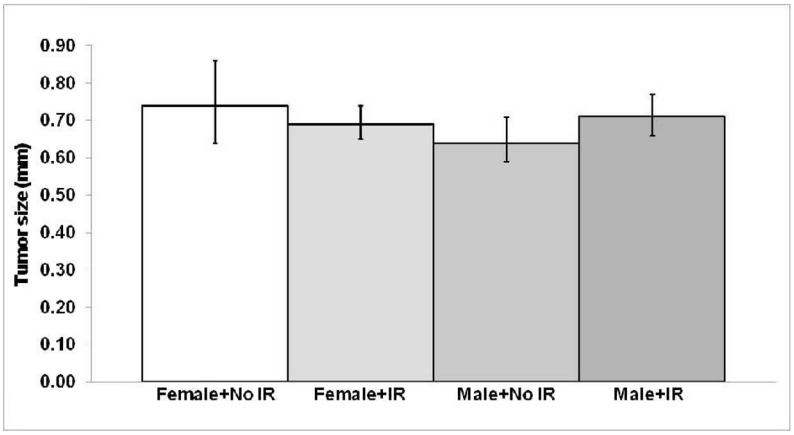

FIG. 5.

Comparison of the mean tumor size (± 95% CI) for female and male mice expressing the Ki-*ras*^{G12C} gene with and without exposure to CT radiation at 1 year of age (9 months postirradiation). $P > 0.3$ for all comparisons.

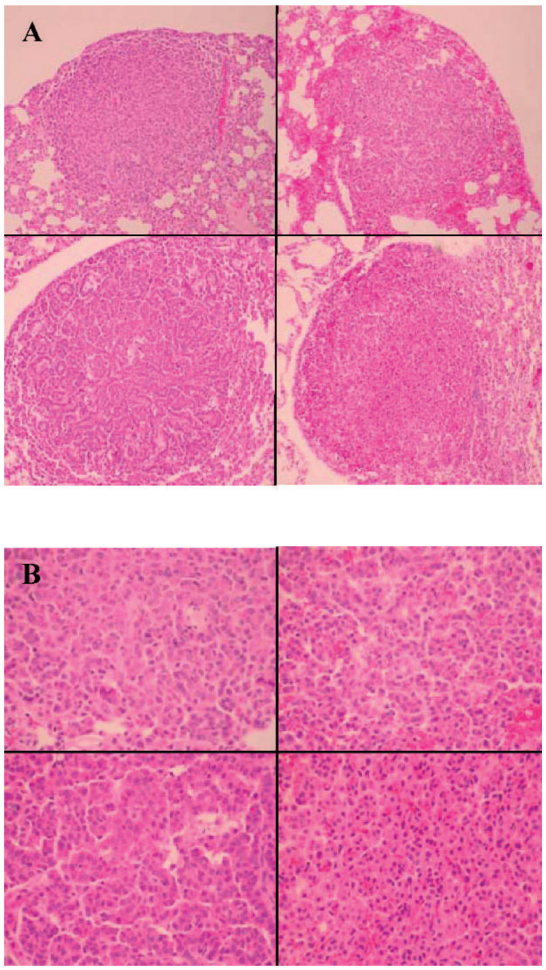

FIG. 6.

Panel A: Top left: DOX + No IR (ionizing radiation); top right: DOX + 80 mGy; bottom left: DOX + 120 mGy; bottom right: DOX + 160 mGy. At a magnification of 10×, after hematoxylin and eosin staining, all four lesions appear similar, being composed of a well-circumscribed, nonencapsulated, closely spaced collection of plump epithelial cells with little morphological variation. Panel B: Top left: DOX + No IR; top right: DOX + 80 mGy; bottom left: DOX + 120 mGy; bottom right: DOX + 160 mGy. At a magnification of 40×, similar cellular morphology for all four lesions can be seen. The lesions are composed of uniform cells with 10–12-μm-diameter round basophilic nuclei with coarsely clumped chromatin, often without nucleoli, and abundant eosinophilic cytoplasm. Mitoses are rare to absent in these lesions.